



### **Science Arts & Métiers (SAM)**

is an open access repository that collects the work of Arts et Métiers Institute of Technology researchers and makes it freely available over the web where possible.

This is an author-deposited version published in: <https://sam.ensam.eu>  
Handle ID: <http://hdl.handle.net/10985/7514>

#### **To cite this version :**

Benjamin ABRIVARD, Etienne PESSARD, Franck MOREL, Philippe DELHAYE, Benjamin GERIN  
- The Effect of microstructural heterogeneities on the fatigue behaviour of 22MnB5 sheet steel -  
In: 13th International Spring Meeting SF2M, France, 2013-05-22 - JIP2013 - Proceedings of the  
conference - 2013

Any correspondence concerning this service should be sent to the repository

Administrator : [scienceouverte@ensam.eu](mailto:scienceouverte@ensam.eu)



# The Effect of microstructural heterogeneities on the fatigue behaviour of 22MnB5 sheet steel

<sup>a-b</sup> B. ABRIVARD, <sup>a</sup> E. PESSARD, <sup>a</sup> F. MOREL, <sup>b</sup> P. DELHAYE, <sup>a</sup> B. GERIN

<sup>a</sup> LAMPA, Arts et Métiers ParisTech, Angers 49035, France

<sup>b</sup> Renault SAS, Le Mans 72086, France

**Abstract** This work deals with the effect of heat treatment on the fatigue strength of a rear axial beam and aims to propose a methodology suitable and reliable for fatigue design. The rear axial beam is made of sheet metal (22MnB5); the initial microstructure is ferrite-pearlitic and martensitic after the treatment. A vast experimental campaign has been undertaken to investigate the behaviour and more specially the fatigue damage mechanisms observed (with material treated and no treated) under different loading conditions: tension and shear test with different load ratios. To test a sheet on shearing an original test is also used.

SEM observations of fatigue failure surfaces, for both heat treated and non-treated specimens, show that the fatigue cracks initiate from inclusions for the specimens loaded in tension. The experiments show that the damage mechanism depends on the applied loading condition: for shear loadings no inclusions are observed at the crack initiation site.

A probabilistic approach using the weakest link concept is used to model the fatigue. This approach leads naturally to a probabilistic Kitagawa type diagram, which in this case explains the relationship between the influence of the heat treatment and the microstructural heterogeneities.

## 1 INTRODUCTION

The 22MnB5 steel, commercially referred to as Usibor 1500 by Arcelor Mittal, has been developed with the aim of reducing the mass of structural components used in the automotive industry. This material is obtained by hot rolling and is characterised by excellent quenchability.

The good quenchability of Boron steels can be taken advantage of by using the Hot Forming Die Quenching process (HFDQ), whereby the sheet metal is austenized and subsequently stamped in a cooled die. [1] To control this process, much research has been devoted to the characterization of the thermo-mechanical behaviour of boron steels [2, 3].

Considerable progress has been made concerning the HFDQ process and it is now possible to vary the final microstructure of a component by optimizing the way in which the tooling is cooled. Some structural components, such as a B-pillar, may benefit from regions that have a lower strength and greater ductility for improved crash performance [4].

Another method of obtaining a heterogeneous microstructure is to manufacture the product by conventional sheet metal forming processes and then to locally quench zones of the component by induction heating. The rear axial beam used in Renault vehicles is a good example of the usefulness of this method. As the axial beam is principally subject to torsional loads, highly loaded zones can be identified. It is therefore, a priori, not necessary to fully heat treat the entire component as a local heat treatment in certain zones could significantly reduce the manufacturing time.

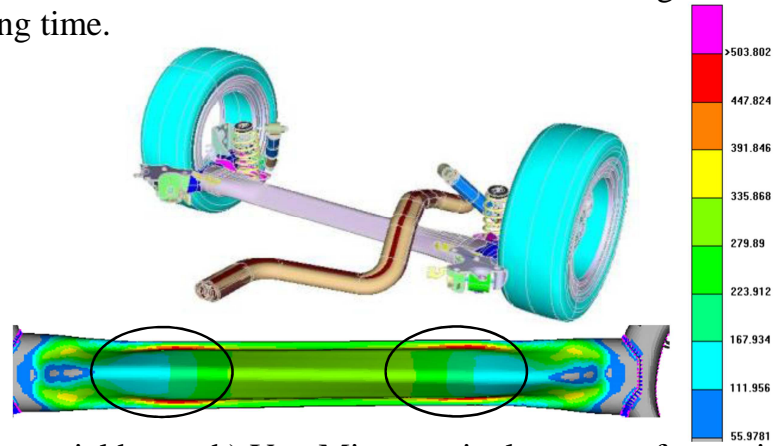


Figure 1: a) rear axial beam, b) Von Mises equivalent stress for torsion loads (from an elastic simulation)

The objective of this work is to propose a fatigue criterion that is capable of explicitly taking into account the effect of the heat treatment. The results of an experimental campaign to characterize the fatigue behaviour of heat treated and non-treated 22MnB5 steel under different cyclic stress states are presented. After an analysis of the failure surfaces, a probabilistic approach to take into account the combined effect of alumina inclusions and the heat treatment on the fatigue behaviour is developed.

## 2 THE MATERIAL, 22MNB5 AND EXPERIMENTAL PROCEDURE

### THE MATERIAL

The material studied in this work is a ferrito-pearlitic steel commercially referred to as Usibor 1500 and is used to reduce the mass of structural components and reinforcements used in the automotive industry. Its chemical composition is given in Table 1. The material is produced in the form of rolled sheets.

Table 1: Chemical composition of the 22MnB5

Element	C	Mn	Si	P	S	Al	Cr	B	Ti	N	Mo
Weight (%)	<b>0.206</b>	<b>1.191</b>	0.264	0,019	0,007	0.02	0.199	<b>0,002</b>	0.02	-	0,003

The material is isotropic in terms of its mechanical behaviour and its mechanical properties are presented in Table 2. The heat treatment consists of an austenitization at 950 °C for 6 minutes, and then quenching in oil. SEM (Scanning Electron Microscope) observations show a ferrito-pearlitic microstructure in its initial state and martensitic after the heat treatment.

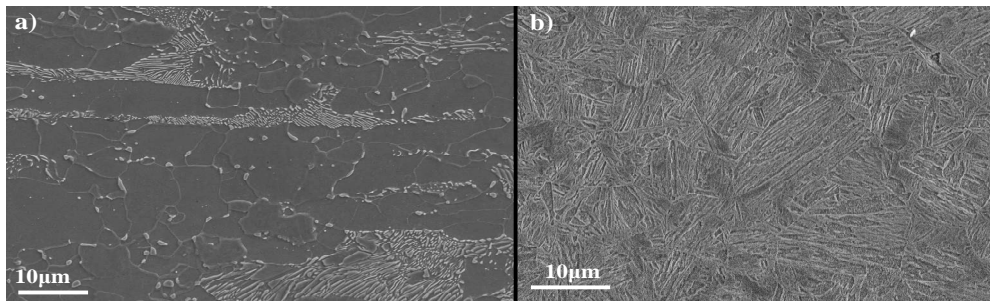


Figure 2: Microstructure of the 22MnB5 steel, a) in its initial state, b) after the heat treatment

Table 2: Mechanical Properties of the 22MnB5 steel

	Ultimate Tensile stress (MPa)	Yield stress (MPa)	Tensile elongation (%)	Superficial hardness HV20
initial state	480	320 - 420	20	180
After heat treatment	1300 - 1650	1000 - 1250	4,5	530

### FATIGUE TEST

For the untreated material, Push-pull ( $R=-1$  and  $R=0,1$ ) fatigue tests were performed using a vibrophore Rumul testing machine at a frequency of approximately 72 Hz. The fatigue limits were evaluated using the staircase method, at  $2 \times 10^6$  cycles using ten specimens per condition.

To define the shearing fatigue limit of the sheet material, an original fatigue test set-up was developed. It is based on the work of [5]. Using a servo-hydraulic fatigue testing machine and the specimen geometry shown in the figure below, it is possible to generate a cyclic pure shear stress state in an area of about 10mm in diameter (see Figure 3).

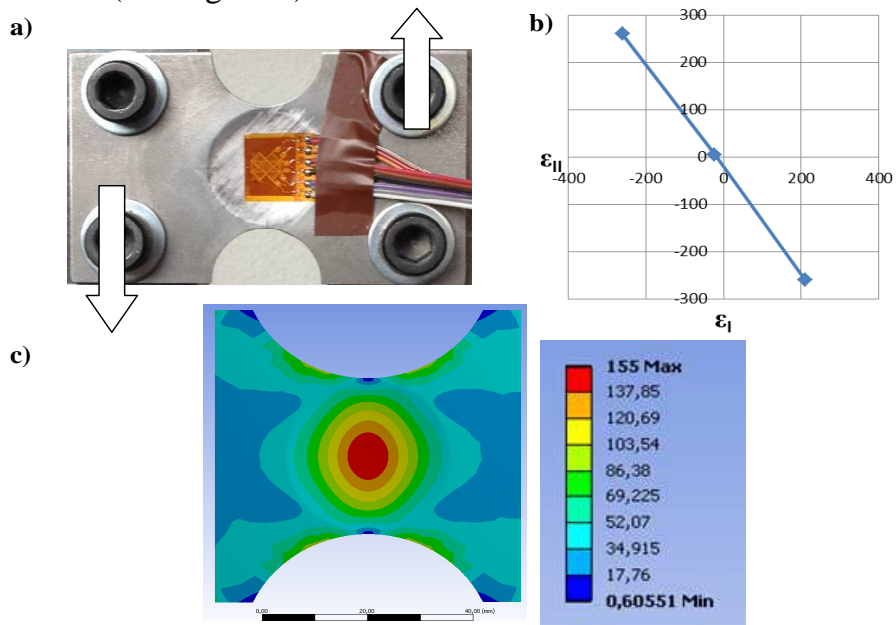


Figure 3: a) Picture of the tool b) Evolution of the two principal deformations during a static loading of tension-compression c) Von Mises Criterion from an elastic simulation (MPa)

With this system, the test frequency is limited. Hence, in order to estimate the high cycle fatigue strength, an accelerated method has been used, that is the self-heating method. These shearing tests were conducted at 10 Hz for load ratios  $R = -1$  and  $R = 0.1$ , a single type T thermocouple is fixed to the specimen surface via adhesive tape to measure the temperature. Blocks of 5000 cycles were applied. To estimate the average fatigue limit, the iteration empirical procedure developed by Cura et al. [10] is used.

### 3 FATIGUE TEST RESULTS AND FRACTURE SURFACES

Table 3 summarised the results of the fatigue test campaign.

Table 3: Fatigue results obtained on the 22MnB5 using staircase method and Self Heating Method (SH test)

		Uniaxial tensile tests	Shear Test
Before Heat Treatment	R=-1	$\sigma=265\pm 5\text{MPa}$	$\tau=180\text{MPa}$ (S.H.test)
	R=0,1	$\sigma=230\pm 6\text{MPa}$	$\tau=156\text{MPa}$ (S.H.test)
After Heat Treatment	R=-1	$\sigma=626\text{MPa}$ (S.H.test)	x
	R=0,1	$\sigma=400\pm 8\text{MPa}$ $\sigma=394\text{MPa}$ (S.H.test)	x

For the heat treated and non-treated materials, when subject to uniaxial tensile cyclic loads ( $R = 0.1$  and  $R = -1$ ) fatigue crack initiation most often occurs at alumina inclusions ( $\text{Al}_2\text{O}_3$ ). The average size of these inclusions is of the order of 40 micrometers, this value is based on measurement realised on 10 fracture surfaces.

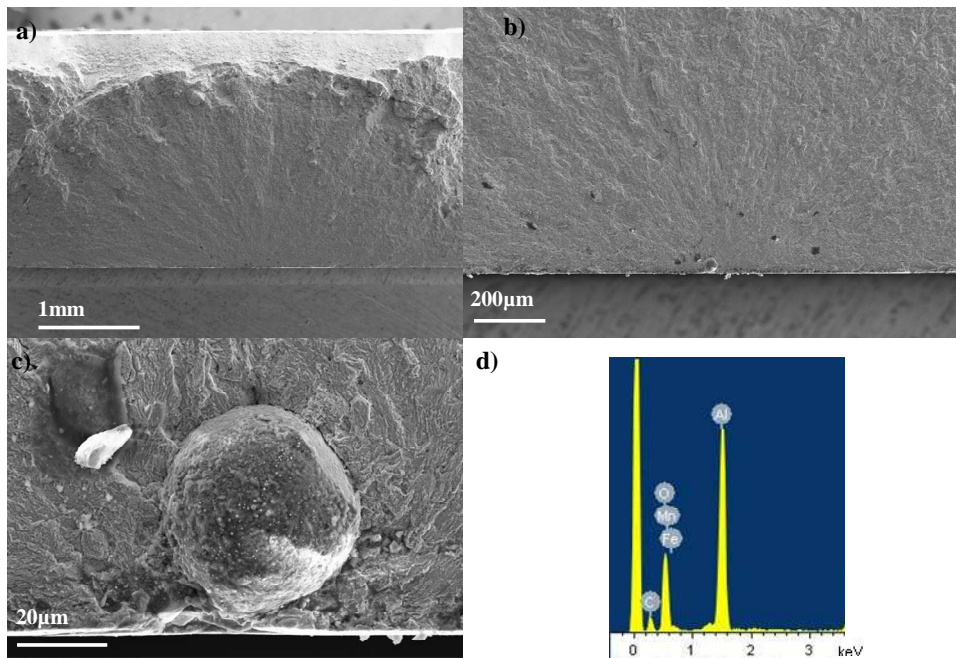


Figure 4: a),b),c) Typical failure surfaces, d) Chemical composition of an inclusion analysed by energy dispersive X-ray spectroscopy

Surface observations of shear specimens shows micro-cracks oriented at  $0^\circ$  and  $90^\circ$  to the specimen axis. This corresponds to the “classical” fatigue crack initiation mechanism in which micro-cracks form on a critical plane (or plane of

greatest shear stress amplitude. SEM observations of the failure surfaces (Fig. 6 b-c) show that the crack initiation sites are not associated with the presence of non-metallic inclusions.

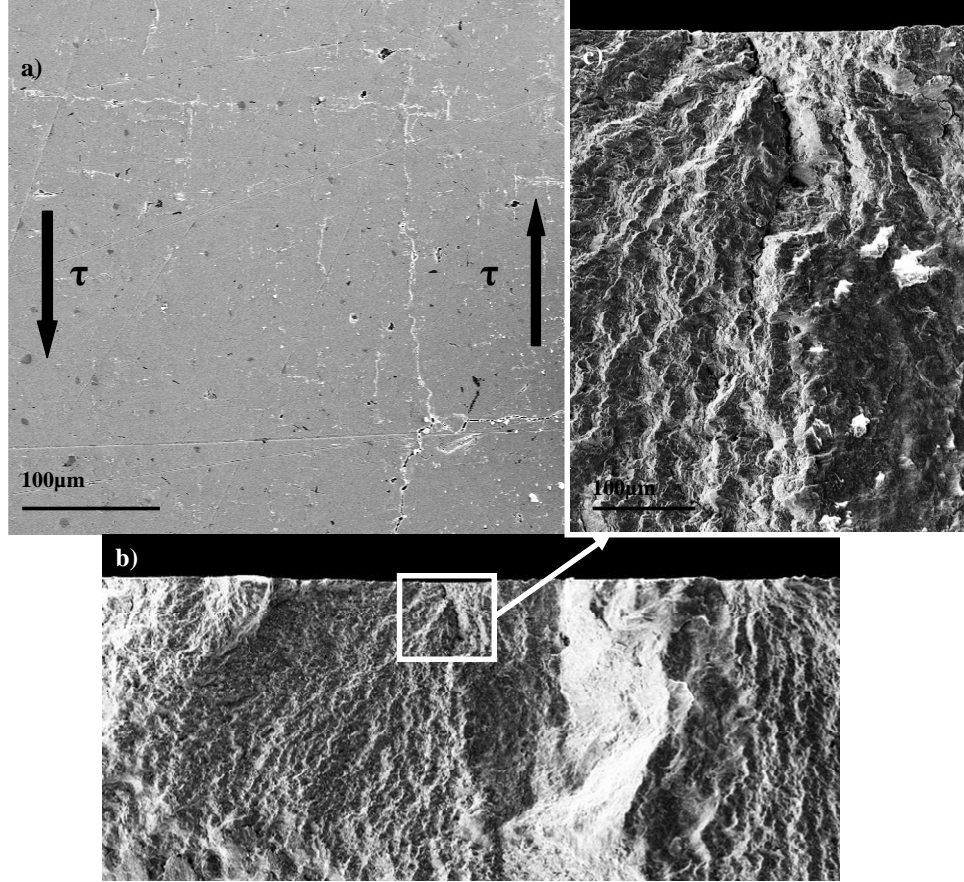


Figure 6: a) Observation on the surface of the a shear specimen showing crack initiating in the material matrix at 0° and 90° to the specimen axis, b-c) failure surfaces of the shear test

#### 4 ANALYSIS

Figure 6 shows the results presented in the form of a Dang Van diagram [7]. This high cycle multiaxial fatigue criterion is a critical plane type criterion that is expressed as a linear combination of the shear stress amplitude on the critical plane and of the maximum hydrostatic stress. The fatigue limit values for the non-treated material form a straight line in this diagram. This line corresponds to the Dang Van criterion, usually used for ductile materials.

Given the hardness of our material and the average defect size, it is possible to use the Murakami [8] criterion to predict fatigue limits for each loading condition. These predictions are plotted in Figure 7. The Murakami [8] criterion uses the parameter  $\sqrt{area}$  (where *area* is the projected area of a defect) and the hardness to define the fatigue strength via the following equation:

$$\sigma_w = \frac{A(H_v + 120)}{(\sqrt{area})^{1/6}} \left( \frac{1-R}{2} \right)^\alpha \quad (1)$$

Where  $\alpha = 0.226 + H_v \times 10^{-4}$  and  $A = 1.43$  or  $1.56$  for surface and internal defects, respectively for torsional loads and surface defects, the fatigue strength can be expressed as:

$$\sigma_w = \frac{0.93(H_v + 120)}{F(b/a)(\sqrt{area})^{1/6}} \left( \frac{1-R}{2} \right)^\alpha \quad (2)$$

where  $F(b/a) = 0.8397$  for spherical defects.

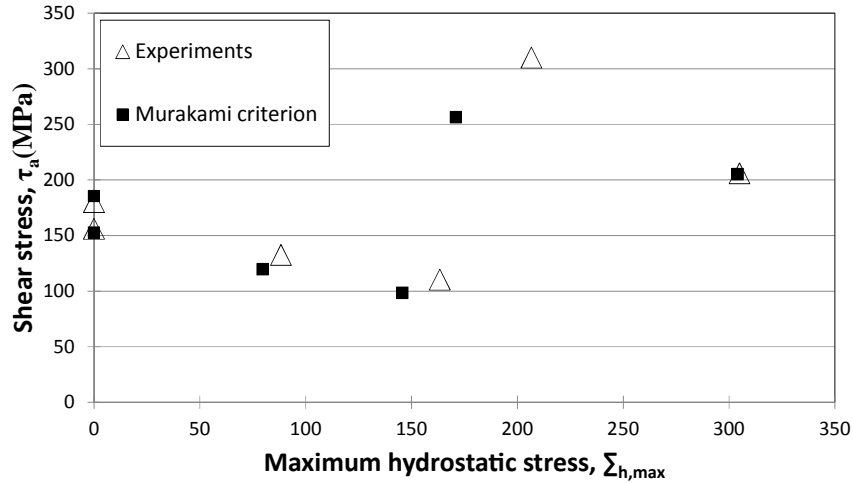


Figure 5: Dang Van diagram, showing the Murakami predictions and the corresponding data for the 22MnB5 steel

It can be seen that the Murakami criterion is able to accurately predict the fatigue limit of the untreated material in tension and shear with  $R=0.1$  and  $R=-1$ . This result is surprising because despite the fact that the damage mechanism observed in shear is not associated with the presence of a defect, the Murakami criterion results in good predictions. Concerning the heat treated material, the Murakami criterion is however less accurate for tensile loads with a  $R$ -ratio of 0.1. This hypothesis, of the existence of two fatigue damage mechanisms, depending on the type of loading condition, has been previously verified [9,10] and will be the basis of the proposed modelling approach.

The proposed modelling framework is a flexible way of taking into account multiple, coexisting, fatigue damage mechanisms via the combination of two appropriate high cycle fatigue criteria. One criterion to model fatigue damage associated with crack initiation and a second for crack propagation (or crack arrest).

## 5 A PROBABILISTIC MULTIAXIAL FATIGUE CRITERION THAT CAN TAKE INTO ACCOUNT THE HEAT TREATMENT EFFECT

In order to model both fatigue crack initiation and propagation, the Crossland [11] and Murakami [11] models have been chosen. The threshold defined by each one of these criteria is then re-defined in terms of a Weibull distribution, giving a failure probability caused by each of these mechanisms.

The total probability of survival of the component is defined by applying the weakest link hypothesis. It is obtained by multiplying the two survival probabilities from the two different observed mechanisms:

	Mechanism 1	Mechanism 2
threshold	$\sigma_{eq} < \sigma_{th}$	$\Delta K < \Delta K_{th}$
Probability density function	$f_{01}(\sigma_{th}) = \frac{m_1}{\sigma_{th01}} \left( \frac{\sigma_{th}}{\sigma_{th01}} \right)^{m_1-1} \exp\left(-\left(\frac{\sigma_{th}}{\sigma_{th01}}\right)^{m_1}\right)$	$f_{02}(\sigma_{th}) = \frac{m_2}{\Delta K_{th02}} \left( \frac{\Delta K_{th}}{\Delta K_{th02}} \right)^{m_2-1} \exp\left(-\left(\frac{\Delta K_{th}}{\Delta K_{th02}}\right)^{m_2}\right)$
Failure probability	$P_{F_1} = 1 - \exp\left[-\frac{1}{S_{01}} \int_{S_{\Omega 1}} \left(\frac{\sigma_{eq}}{\sigma_{th01}}\right)^{m_1} dS\right]$	$P_{F_2} = 1 - \exp\left[-\frac{1}{S_{02}} \int_{S_{\Omega 2}} \left(\frac{\Delta K}{\Delta K_{th02}}\right)^{m_2} dS\right]$
Total failure probability	$P_F = 1 - \exp\left\{-\left[\frac{S_{\Omega 1}}{S_{01}} \left(\frac{\sigma_{eq}}{\sigma_{th01}}\right)^{m_1} + \frac{S_{\Omega 2}}{S_{02}} \left(\frac{\Delta K}{\Delta K_{th02}}\right)^{m_2}\right]\right\}$	

For example, for traction-compression loads, the Crossland [11] criterion can be written as:

$$\sigma_{eq} = \sqrt{J_{2,a}} + k\sigma_{H,\max} = \left(\frac{1}{\sqrt{3}} + \frac{2k}{3(1-R)}\right)\sigma_{I,a} \quad (3)$$

and the Murakami criterion can be written as :

$$\Delta K = 0.65\sigma_{I,a}\sqrt{\pi\sqrt{area}} \quad \text{and} \quad \Delta K_{th} = 3.3 \times 10^{-3}(H_v + 120)(\sqrt{area})^{1/3} \left(\frac{1-R}{2}\right)^\alpha \quad (4)$$

By assuming that the scatter is the same for both mechanisms,  $m = m_1 = m_2$  that there is no scale effect  $\left(\frac{S_{\Omega 1}}{S_{01}} = \frac{S_{\Omega 2}}{S_{02}} = 1\right)$  and the defects have a spherical shape, the traction-compression fatigue limit can be written as:

$$\sigma_{I,a}(P_f, a) = \left[ \frac{\ln\left(\frac{1}{1-P_f}\right)}{\left(\frac{1}{\sqrt{3}} + \frac{2k}{3(1-R)}\right)^m + \left(\frac{a^{1/6}}{C'_{th02} \left(\frac{1-R}{2}\right)^\alpha}\right)^m} \right]^{\frac{1}{m}} \quad (5)$$

Where  $\sigma'_{th01}$  and  $C'_{th02}$  are the material parameters for the thresholds associated with the two mechanism.  $k$  is the Crossland parameter that takes into account the hydrostatic stress. Plotting the fatigue limit as a function of the defect size it is possible to obtain a Kitagawa type diagram (Figure 7)

In order to take into account the effect of the heat treatment, it is necessary to make both thresholds  $\sigma'_{th01}$  and  $C'_{th02}$  a function of the heat treatment. As well, for the Murakami criterion, it is proposed to make both thresholds depend on the hardness.

$$\sigma'_{th01} = C_{01}(H_v + 120) \quad \text{and} \quad C'_{th02} = C_{02}(H_v + 120) \quad (6)$$

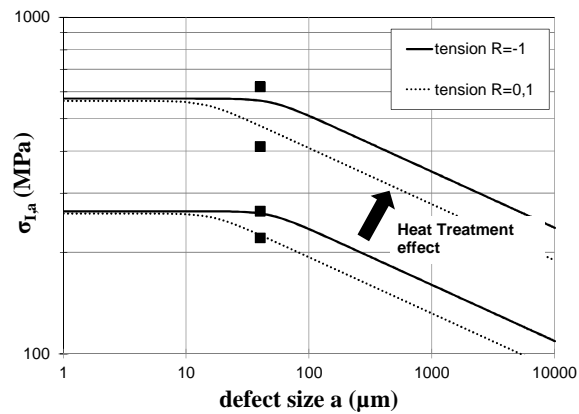


Figure 6: Effect of the heat treatment on the Kitagawa diagram on the 22MnB5

This is a strong assumption that is proposed in order to demonstrate the possibilities of the proposed model. The aim is to develop an approach that is both phenomenological and empirical, which can be applied to the industrial problem of applying a local heat, the results of which are currently measured in terms of hardness. It is necessary to undertake a larger testing program in order to identify each one of these relationships. The predictions from the proposed model are shown in a Kitagawa's diagram (Figure 7).

## 6 CONCLUSION

The fatigue behaviour of the 22MnB5 steel has been characterized for different loading conditions and heat treatments. For this, an original shearing test setup has been employed to determine the fatigue behaviour of the 22MnB5 steel in shear. An analysis of the fatigue failure surfaces show that the crack initiation mechanism depends on the type of applied load. An original modelling approach has been developed to take into account the evolution of the fatigue behaviour depending on the applied heat treatment.

## 7 REFERENCES

- [1] H. Karbasian, A.E. Tekkaya, A review on hot stamping, *Journal of Materials Processing Technology* 210 (2010) 2103–2118.
- [2] H. Liu, Hot formation quality of high strength steel BR1500HS for hot stamping without cooling system, *Trans. Nonferrous Met. Soc. China* 22(2012) s542–s547.
- [3] A. Bardelcik, Effect of cooling rate on the high strain rate properties of boron steel, *International Journal of Impact Engineering* 37 (2010) 694–702.
- [4] M. Merklein, Investigation of the thermo-mechanical properties of hot stamping steels, *Journal of Materials Processing Technology* 177 (2006) 452–455.
- [5] A. Galtier et B. Weber, *Fatigue tests on thin sheet materials*, fatigue design 2005.
- [6] F. Cura, G. Curti, R. Sesana, *Int. J. Fatigue* 27 (2005) 453–459.
- [7] K. DangVan, *Sur la résistance en fatigue des métaux*, *Sci Tech Armement*, 1973, 47
- [8] Y. Murakami *Metal fatigue effects of small defects and non-metallic inclusions*, Elsevier 2002
- [9] E. Pessard, F. Morel, A. Morel, D. Bellett, Modelling the role of non-mettalic inclusions on the anisotropic fatigue behaviour of forged steel, *Int. J. Fatigue* 33-4 (2011) 568-577
- [10] I. Koutiri, D. Bellett, F. Morel, E. Pessard, A probabilistic model for the high cycle fatigue behaviour of cast aluminium alloys subject to complex loads, *Int. J. Fatigue* 47 (2013) 137-147
- [11] B. Crossland, *Int. Conf. on Fatigue of Metals*, 1956, London